Plug-and-Play Control and Optimization in Microgrids

Florian Dörfler, John W. Simpson-Porco, and Francesco Bullo

Abstract— A hierarchical layering of primary, secondary, and tertiary control is the standard operation paradigm for bulk power systems. Similar hierarchical decision architectures have been proposed for microgrids. However, the control objectives in microgrids must be achieved while allowing for robust plug-and-play operation and maximal flexibility, without hierarchical decision making, time-scale separations, and central authorities. Here, we explore control and optimization strategies for the three decision layers and illuminate some possibly-unexpected connections and dependencies among them. Our analysis builds upon first-principle models and decentralized droop control. We investigate distributed architectures for secondary frequency regulation and find that averaging-based distributed controllers using communication among the generation units offer the best combination of flexibility and performance. We further leverage these results to study constrained AC economic dispatch in a tertiary control layer. We show that the minimizers of the economic dispatch problem are in one-to-one correspondence with the set of steady-states reachable by droop control. This equivalence results in simple guidelines to select the droop coefficients, which include the known criteria for load sharing.

I. INTRODUCTION

With the goal of integrating distributed renewable generation and energy storage systems, the concept of a *microgrid* has recently gained popularity [2]–[5]. Microgrids are low-voltage distribution networks composed of distributed generation, storage, load, and managed autonomously from the larger transmission network. Microgrids are able to connect to a larger power system, but are also able to island themselves and operate independently. The sources in a microgrid generate either DC or variable frequency AC power, and are interfaced with an AC grid via power electronic DC/AC *inverters*. Through these inverters, cooperative actions must be taken to ensure stability, power balance, load sharing, and economic operation. A variety of decision and control architectures — ranging from centralized to fully decentralized — have been proposed to address these challenges [5]–[7].

In conventional bulk power systems, the different control tasks are separated in their time scales and aggregated into a hierarchy. The foundation of this hierarchy, termed *primary control*, must rapidly balance generation and demand, while sharing the load, synchronizing the AC voltage frequencies, and stabilizing their magnitudes. This is accomplished via decentralized *droop* control balancing of power injections and voltage frequencies and magnitudes. Droop controllers

F. Dörfler is with the Department of Electrical Engineering, University of California Los Angeles. Email: `dorfler@seas.ucla.edu`. J. W. Simpson-Porco and F. Bullo are with the Mechanical Engineering Department, University of California Santa Barbara. Email: {`johnwsimpsonporco,bullo`}`@engineering.ucsb.edu`.

induce steady-state errors in frequency and voltage magnitudes, which are corrected in a *secondary control* layer. A few selected generators then perform secondary control by balancing generation with load and inter-area power transfers. Termed *automatic generation control* (AGC), this architecture is based on centralized integral control and operates on a slower time scale than primary control [8]. The operating point stabilized by primary/secondary control is scheduled in a *tertiary* control layer to dispatch the generation to minimize operational costs or to establish a fair load sharing. Typically, an economic dispatch is optimized offline, in a centralized fashion, using precise load forecasts [9].

While this hierarchical architecture can be adapted from the transmission level to microgrids, the control challenges and architecture limitations imposed by the microgrid framework are diverse and daunting. The high penetration of renewables, the low levels of inertia, and the poorly predictable load profiles lead to volatile dynamics requiring fast control actions. On the other hand, the distributed nature of microgrids preclude centralized control strategies of any kind. Microgrid controllers must be able to adapt in real time to unknown and variable loads and network conditions. In short, the three layers of the control hierarchy for microgrids must allow for as close to plug-and-play operation as possible, be either distributed or completely decentralized, and operate seamlessly without a pre-imposed separation of time scales.

For these reasons, recent research efforts aim at connecting the three different decision layers – in load control, in AGC, and in microgrids. Primary and secondary control can be achieved in a fully decentralized fashion [10] at the cost of steady-state deviations from the desired power injection profile. Thus, distributed controllers merging primary and secondary control have been proposed based upon continuous-time averaging with all-to-all [11]–[13] or nearest-neighbor [14]–[16] communication. The tertiary optimization layer can be merged with the primary and secondary control layer based on continuous-time optimization approaches [1], [17]–[22]. Similar discrete-time approaches are based on game-theoretic ideas [23] or discrete-time averaging algorithms [24], [25].

All of the above references share the following characteristics: (i) *Averaging-based control strategies* are employed to maintain the desired operating point despite an unknown load profile. (ii) All approaches incorporating the tertiary optimization layer essentially rely upon the following insight termed *economic dispatch criterion* [9]: all marginal utilities must be identical in a lossless network. On the other hand, all of the above strategies make use of physical models ranging from nonlinear differential-algebraic models to the absence of models. Likewise, the proposed control strategies are of

different communication and computational complexities.

In this paper, we present a comprehensive modeling framework for microgrids with heterogenous components and different control tasks (Section II). Building on decentralized primary droop control, we study a first-principle, nonlinear, and differential-algebraic model. In Section III, we investigate the limitations of droop control and show that the set of steady-states reachable via droop control are in one-to-one correspondence with the set of feasible injection setpoints.

In Section IV, we first discuss the limitations of decentralized secondary integral control akin to AGC. Next, we review the distributed averaging-based PI (DAPI) control strategy [14], [15], [18], [21] the effectiveness of which has been confirmed experimentally [16]. We show that DAPI control successfully regulates the frequency, maintains the injections and stability properties of the primary control in presence of unknown loads, and does not require any separation of time scales.

In Section V, we study tertiary control policies that minimize an economic dispatch problem. We leverage a recently discovered relation between AC and DC power flows [26], [27] and show that the minimizers of the nonlinear and non-convex AC economic dispatch optimization problem are in one-to-one correspondence with the minimizers of a convex DC dispatch problem. Our next result shows a surprising symbiotic relationship between primary/secondary control and tertiary. We show that the minimum of the AC economic dispatch can be achieved by decentralized droop control. Conversely, every droop controller results in a steady-state which is the minimizer of some AC economic dispatch. We deduce, among others, that the optimal droop coefficients are inversely proportional to the marginal cost of generation.

In Section VI, we illustrate the performance and robustness of our controllers with a simulation study of the IEEE 37 distribution network. Finally, Section VII concludes the paper. The remainder of this section introduces some preliminaries.

Preliminaries and Notation

Vectors: Given a finite set $\mathcal{V}$, let $|\mathcal{V}|$ denote its cardinality. Given a finite index set $\mathcal{I}$ and a real-valued one-dimensional array $\{x_1, \ldots, x_{|\mathcal{I}|}\}$, the associated vector and diagonal matrix are $x \in \mathbb{R}^{|\mathcal{I}|}$ and $\mathrm{diag}(\{x_i\}_{i \in \mathcal{I}}) \in \mathbb{R}^{|\mathcal{I}| \times |\mathcal{I}|}$. Let $\mathbf{1}_n$ and $\mathbf{0}_n$ be the n-dimensional vectors of unit and zero entries. We denote the diagonal vector space $\mathrm{Span}(\mathbf{1}_n)$ by $\mathbb{1}_n$ and its orthogonal complement by $\mathbb{1}_n^\perp \triangleq \{x \in \mathbb{R}^n : \mathbf{1}_n^T x = 0\}$.

Algebraic graph theory: We denote by $G(\mathcal{V}, \mathcal{E}, A)$ an undirected and weighted graph, where $\mathcal{V}$ is node set, $\mathcal{E} \subseteq \mathcal{V} \times \mathcal{V}$ is the edge set, and $A = A^T \in \mathbb{R}^{|\mathcal{V}| \times |\mathcal{V}|}$ is the *adjacency matrix*. If a number $\ell \in \{1, \ldots, |\mathcal{E}|\}$ and an arbitrary direction are assigned to each edge, the *incidence matrix* $B \in \mathbb{R}^{|\mathcal{V}| \times |\mathcal{E}|}$ has non-zero components $B_{k\ell} = 1$ if node k is the sink node of edge ℓ and $B_{k\ell} = -1$ if node k is the source node of edge ℓ. The *Laplacian matrix* is $L \triangleq B\mathrm{diag}(\{a_{ij}\}_{\{i,j\} \in \mathcal{E}})B^T$. If the graph is connected, then $\ker(B^T) = \ker(L) = \mathbb{1}_{|\mathcal{V}|}$. For acyclic graphs, $\ker(B) = \emptyset$, and for every $x \in \mathbb{1}_{|\mathcal{V}|}^\perp$ there is a unique $\xi \in \mathbb{R}^{|\mathcal{E}|}$ satisfying *Kirchoff's Current Law* (KCL) $x = B\xi$, where x and ξ correspond to nodal injections and edge flows, respectively.

Geometry on the n-torus: The set $\mathbb{S}^1$ denotes the *circle*, an *angle* is a point $\theta \in \mathbb{S}^1$, and an *arc* is a connected subset of $\mathbb{S}^1$. Let $|\theta_1 - \theta_2|$ be the *geodesic distance* between $\theta_1, \theta_2 \in \mathbb{S}^1$. The *$n$-torus* is $\mathbb{T}^n = \mathbb{S}^1 \times \cdots \times \mathbb{S}^1$. For $\gamma \in [0, \pi/2[$ and a graph $G(\mathcal{V}, \mathcal{E}, \cdot)$, let $\overline{\Delta}_G(\gamma) = \{\theta \in \mathbb{T}^{|\mathcal{V}|} : \max_{\{i,j\} \in \mathcal{E}} |\theta_i - \theta_j| \leq \gamma\}$ be the closed set of angle arrays $\theta = (\theta_1, \ldots, \theta_n)$ with neighboring angles θ_i and θ_j, $\{i, j\} \in \mathcal{E}$ no further than γ apart. Let $\Delta_G(\gamma)$ be the interior of $\overline{\Delta}_G(\gamma)$.

II. MICROGRIDS AND THEIR CONTROL CHALLENGES

A. Microgrids and AC Circuits

We model a microgrid as a synchronous linear circuit with admittance matrix $Y \in \mathbb{C}^{n \times n}$. The associated connected, undirected, and complex-weighted graph is $G(\mathcal{V}, \mathcal{E}, A)$ with node set (or buses) $\mathcal{V} = \{1, \ldots, n\}$, edge set (or branches) $\mathcal{E} \subset \mathcal{V} \times \mathcal{V}$, and symmetric weights (or admittances) $a_{ij} = -Y_{ij} = -Y_{ji} \in \mathbb{C}$ for each $\{i, j\} \in \mathcal{E}$. We restrict ourselves to the *acyclic* (also called radial) topologies prevalent in low-voltage distribution networks. To each node $i \in \mathcal{V}$, we associate a power injection $P_{\mathrm{e},i} + \sqrt{-1}Q_{\mathrm{e},i} \in \mathbb{C}$ and a voltage phasor $V_i = E_i e^{\sqrt{-1}\theta_i} \in \mathbb{C}$ corresponding to the magnitude $E_i > 0$ and the phase angle $\theta_i \in \mathbb{S}^1$ of a harmonic voltage signal. For *inductive lines*, the admittance matrix $Y \in \mathbb{C}^{n \times n}$ is purely imaginary, and the active/reactive injections are

$$P_{\mathrm{e},i} = \sum_{j=1}^n \mathfrak{Im}(Y_{ij})E_i E_j \sin(\theta_i - \theta_j), \quad i \in \mathcal{V}, \quad (1a)$$

$$Q_{\mathrm{e},i} = -\sum_{j=1}^n \mathfrak{Im}(Y_{ij})E_i E_j \cos(\theta_i - \theta_j), \quad i \in \mathcal{V}. \quad (1b)$$

We adopt the standard *decoupling approximation* [4] where all voltage magnitudes E_i are constant in the active power injections (1a) and $P_{\mathrm{e},i} = P_{\mathrm{e},i}(\theta)$. By continuity and exponential stability, our results are robust to bounded voltage dynamics [15], [26], which we illustrate via simulations.

We partition the buses into loads and inverters, $\mathcal{V} = \mathcal{V}_L \cup \mathcal{V}_I$, and denote their cardinalities by $n \triangleq |\mathcal{V}|$, $n_L \triangleq |\mathcal{V}_L|$, and $n_I \triangleq |\mathcal{V}_I|$. Each load $i \in \mathcal{V}_L$ demands a constant amount of active power $P_i^* \in \mathbb{R}$ and satisfies the power flow equation

$$0 = P_i^* - P_{\mathrm{e},i}(\theta), \quad i \in \mathcal{V}_L. \quad (2)$$

We refer to the buses $\mathcal{V}_L$ strictly as *loads*, with the understanding that they can be loads or constant-power sources.

We denote the rating (maximal power injection) of inverter $i \in \mathcal{V}_I$ by $\overline{P}_i \geq 0$. As a necessary feasibility condition, we assume that the total load $\sum_{i \in \mathcal{V}_L} P_i^*$ is a net demand serviceable by the inverters' maximal generation:

$$0 \leq -\sum_{i \in \mathcal{V}_L} P_i^* \leq \sum_{i \in \mathcal{V}_I} \overline{P}_i. \quad (3)$$

After designing inner control loops, an inverter can be regarded as *controllable voltage source* behind a reactance [4].

B. Primary Droop Control

The *frequency droop controller* is the main technique for primary control in microgrids [3]–[7]. At inverter i, the frequency $\dot{\theta}_i$ is controlled to be proportional to the measured (see [4] for details) power injection $P_{\mathrm{e},i}(\theta)$ according to

$$D_i \dot{\theta}_i = P_i^* - P_{\mathrm{e},i}(\theta), \quad i \in \mathcal{V}_I, \quad (4)$$

where $P_i^* \in [0, \overline{P}_i]$ is a *nominal injection setpoint*, and the proportionality constant $D_i \geq 0$ is referred to as the (inverse) *droop coefficient*. In this notation, $\dot{\theta}_i$ is actually the frequency error $\omega_i - \omega^*$, where ω^* is the nominal network frequency.

The droop-controlled microgrid is then described by the nonlinear, differential-algebraic equations (DAE) (2),(4).

Remark 1: **(Extensions).** The model (1),(4) assumes purely inductive lines, which can be justified as the inverter output impedances can be controlled to dominate over the network impedances. Our analysis can be easily extended towards more general networks, including resistive/capacitive lines, constant R/X ratios, and networks with sufficiently uniform R/X ratios. Likewise, all of our results pertaining to equilibria of the model (2),(4) and their local stability properties extend to synchronous machines, inverters with measurement delays, and frequency-dependent loads. We refer to [1] for details and focus on the model (2),(4). $\square$

C. Secondary Frequency Control

If the droop-controlled system (2), (4) settles to a solution with synchronized frequencies, $\dot{\theta}_i(t) = \omega_{\text{sync}} \in \mathbb{R}$ for all $i \in \mathcal{V}$, then summing over all equations (2),(4) yields

$$\omega_{\text{sync}} \triangleq \frac{\sum_{i \in \mathcal{V}} P_i^*}{\sum_{i \in \mathcal{V}_I} D_i} . \tag{5}$$

Notice that ω_{sync} is a *scaled power imbalance* and equals zero if and only if the nominal injections P_i^* are balanced: $\sum_{i \in \mathcal{V}} P_i^* = 0$. Since the loads are generally unknown, it is not possible to schedule the sources to balance them. Likewise, to render ω_{sync} small, the gains D_i cannot be chosen arbitrary large, since the primary control becomes slow and possibly unstable.

To eliminate this frequency error, the primary control (4) needs to be augmented with *secondary control* inputs $u_i(t)$:

$$D_i \dot{\theta}_i = P_i^* - P_{\text{e},i}(\theta) + u_i(t) . \tag{6}$$

If there is a synchronized solution to the secondary-controlled equations (2),(6) with frequency ω_{sync}^* and steady-state secondary control $u_i^* = \lim_{t \to \infty} u_i(t)$, then we obtain

$$\omega_{\text{sync}}^* = \frac{\sum_{i \in \mathcal{V}} P_i^* + \sum_{j \in \mathcal{V}_I} u_i^*}{\sum_{i \in \mathcal{V}_I} D_i} = \omega_{\text{sync}} + \frac{\sum_{j \in \mathcal{V}_I} u_i^*}{\sum_{i \in \mathcal{V}_I} D_i} . \tag{7}$$

Clearly, there are many choices for the inputs u_i^* to achieve the control objective $\omega_{\text{sync}}^* = 0$. However, the inputs u_i^* are typically constrained due to additional performance criteria.

D. Tertiary Operational Control

A tertiary control layer has the objective to minimize an *economic dispatch*, that is, the cost accumulated generation:

$$\underset{\theta \in \mathbb{T}^n, \, u \in \mathbb{R}^{n_I}}{\text{minimize}} \quad f(u) = \sum_{i \in \mathcal{V}_I} \frac{1}{2} \alpha_i u_i^2 \tag{8a}$$

$$\text{subject to} \quad P_i^* + u_i = P_{\text{e},i}(\theta) \qquad \forall \, i \in \mathcal{V}_I, \tag{8b}$$

$$P_i^* = P_{\text{e},i}(\theta) \qquad \forall \, i \in \mathcal{V}_L, \tag{8c}$$

$$|\theta_i - \theta_j| \leq \gamma_{ij}^{(\text{AC})} \qquad \forall \, \{i,j\} \in \mathcal{E}, \tag{8d}$$

$$P_{\text{e},i}(\theta) \in [0, \overline{P}_i] \qquad \forall \, i \in \mathcal{V}_I. \tag{8e}$$

Here, $\alpha_i > 0$ is the marginal cost for source $i \in \mathcal{V}_I$. The decision variables are the angles θ and secondary control inputs u. The non-convex equality constraints (8b)-(8c) are the nonlinear steady-state secondary control equations, the *security constraint* (8d) limits the power flow on each branch $\{i,j\} \in \mathcal{E}$ by $\gamma_{ij}^{(\text{AC})} \in [0, \pi/2[$, and (8e) is a *generation constraint*. Two typical instances of the economic dispatch (8) are as follows: For $P_i^* = 0$, u_i equals $P_{\text{e},i}(\theta)$, and the total generation cost is penalized. For positive nominal generation setpoints $P_i^* > 0$ (e.g., scheduled according to some load forecast), u_i^* is the real-time operating reserve.

III. DECENTRALIZED PRIMARY CONTROL STRATEGIES

A. Symmetries, Synchronization, and Transformations

The microgrid equations (2),(4) feature an inherent *rotational symmetry*: they are invariant under a rigid rotation of all angles. Formally, let $\text{rot}_s(r) \in \mathbb{S}^1$ be the rotation of a point $r \in \mathbb{S}^1$ counterclockwise by the angle $s \in [0, 2\pi]$. For $(r_1, \ldots, r_n) \in \mathbb{T}^n$, define the equivalence class

$$[(r_1, \ldots, r_n)] = \{(\text{rot}_s(r_1), \ldots, \text{rot}_s(r_n)) \in \mathbb{T}^n : s \in [0, 2\pi]\} .$$

Thus, a synchronized solution $\theta^*(t)$ of (2),(4) is part of a one-dimensional connected *synchronization manifold* $[\theta^*]$; or an equilibrium manifold of (2),(4) if $\omega_{\text{sync}} = 0$. Thus, when we refer to a synchronized solution as "stable" or "unique", these properties are to be understood modulo rotational symmetry.

We make use of this rotational symmetry and establish the equivalence of three different problems: stability of synchronized solutions for primary control, stability of equilibria with appropriate constant secondary control inputs u_i, and stability of equilibria in a set of shifted coordinates.

Recall that, in absence of secondary control, ω_{sync} is the scaled power imbalance (5). By transforming to a rotating coordinate frame with frequency ω_{sync}, that is, $\theta_i(t) \mapsto \text{rot}_{\omega_{\text{sync}} t}(\theta_i(t))$ (with slight abuse of notation, we maintain the variable θ), a synchronized solution of (2),(4) is equivalent to an equilibrium of the *shifted control system*

$$0 = \widetilde{P}_i - P_{\text{e},i}(\theta), \qquad i \in \mathcal{V}_L, \tag{9a}$$

$$D_i \dot{\theta}_i = \widetilde{P}_i - P_{\text{e},i}(\theta), \qquad i \in \mathcal{V}_I, \tag{9b}$$

where the *shifted injections* are $\widetilde{P}_i = P_i^*$ for $i \in \mathcal{V}_L$, and $\widetilde{P}_i = P_i^* - D_i \omega_{\text{sync}}$ for $i \in \mathcal{V}_I$. Observe that the shifted injections in (9) are balanced: $\widetilde{P} \in \mathbb{1}_n^\perp$. Equivalently to transforming to a rotating frame with frequency ω_{sync}, we can assume that the secondary control input in (2),(6) takes the constant value $u_i = -D_i \omega_{\text{sync}}$ to arrive at the shifted control system (9). We summarize these observations:

Lemma 3.1: **(Synchronization Equivalences).** The following statements are equivalent:

(i) The primary droop-controlled microgrid (2),(4) possesses a locally exponentially stable and unique synchronization manifold $t \mapsto [\theta(t)] \subset \mathbb{T}^n$ for all $t \geq 0$;

(ii) The secondary droop-controlled microgrid (2),(6) with constant secondary-control input $u_i = -D_i \omega_{\text{sync}}$ for all $i \in \mathcal{V}_I$ possesses a locally exponentially stable and unique equilibrium manifold $[\bar{\theta}] \subset \mathbb{T}^n$;

(iii) The shifted control system (9) possesses a locally exponentially stable and unique equilibrium $[\tilde{\theta}] \subset \mathbb{T}^n$.

If the equivalent statements (i)-(iii) are true, then all systems have the same synchronization manifolds $[\theta(t)] = [\bar{\theta}] = [\tilde{\theta}] \subset \mathbb{T}^n$ and the same power injections $P_e(\theta(t)) = P_e(\bar{\theta}) = P_e(\tilde{\theta})$. Additionally, $\theta(t) = \mathrm{rot}_{\omega_{\mathrm{sync}}t}(\xi_0)$ for some $\xi_0 \in [\bar{\theta}] = [\tilde{\theta}]$.

In light of Lemma 3.1, we restrict the discussion in this section to the shifted control system (9). Observe also that equilibria of (9) are invariant under *constant scaling* of all droop coefficients: if D_i is replaced by $D_i \cdot \beta$ for some $\beta \in \mathbb{R}$, then ω_{sync} changes to $\omega_{\mathrm{sync}}/\beta$. Since the product $D_i \cdot \omega_{\mathrm{sync}}$ remains constant, the equilibria of (9) do not change. Moreover, if $\beta > 0$, then the stability properties of equilibria do not change since time can be rescaled as $t \mapsto t/\beta$.

B. Existence, Uniqueness, & Stability of Synchronization

In vector form, the equilibria of (9) satisfy

$$\widetilde{P} = B\mathcal{A}\sin(B^T\theta), \tag{10}$$

where $\mathcal{A} = \mathrm{diag}(\{\mathfrak{Im}(Y_{ij})E_iE_j\}_{\{i,j\}\in\mathcal{E}})$ and $B \in \mathbb{R}^{|\mathcal{V}|\times|\mathcal{E}|}$ is the incidence matrix. For an acyclic network, $\ker(B) = \emptyset$, and the unique vector of branch flows $\xi \in \mathbb{R}^{|\mathcal{E}|}$ (associated to the shifted injections $\widetilde{P}$) is given by KCL as $\xi = B^\dagger\widetilde{P} = (B^TB)^{-1}B^T\widetilde{P}$. Hence, equations (10) equivalently read as

$$\xi = \mathcal{A}\sin(B^T\theta). \tag{11}$$

Due to boundedness of the sinusoid, a necessary condition for solvability of (11) is $\|\mathcal{A}^{-1}\xi\|_\infty < 1$. The following result shows that this condition is also sufficient and guarantees stability of an equilibrium manifold of (9) [15, Theorem 2].

Theorem 3.2: (**Existence and Stability of Synchronization**). Consider the shifted control system (9). Let $\xi \in \mathbb{R}^{|\mathcal{E}|}$ be the unique vector satisfying the KCL, given by $\xi = B^\dagger\widetilde{P}$. The following two statements are equivalent:

(i) **Synchronization:** there exists an arc length $\gamma \in [0, \pi/2[$ such that the shifted control system (9) possesses a locally exponentially stable and unique equilibrium manifold $[\theta^*] \subset \overline{\Delta}_G(\gamma)$;
(ii) **Flow feasibility:** the power flow is feasible, that is,

$$\Gamma \triangleq \|\mathcal{A}^{-1}\xi\|_\infty < 1. \tag{12}$$

If the equivalent statements (i) and (ii) hold true, then the quantities $\Gamma \in [0, 1[$ and $\gamma \in [0, \pi/2[$ are related uniquely via $\Gamma = \sin(\gamma)$, and $\sin(B^T\theta^*) = \mathcal{A}^{-1}\xi$.

C. Power Flow Constraints and Proportional Load Sharing

While Theorem 3.2 gives the exact stability condition, it offers no guidance on how to select the control parameters (P_i^*, D_i) to achieve a set of desired steady-state power injections. One desired objective is that all sources meet their the actuation constraints $P_{e,i}(\theta) \in [0, \overline{P}_i]$ and share the load in a fair way according to their power ratings [4], [5]:

Definition 1: (**Proportional Load Sharing**). Consider an equilibrium manifold $[\theta^*] \subset \mathbb{T}^n$ of the shifted control system (9). The inverters share the total load *proportionally according to their power ratings* if for all $i, j \in \mathcal{V}_I$,

$$P_{e,i}(\theta^*)/\overline{P}_i = P_{e,j}(\theta^*)/\overline{P}_j. \tag{13}$$

We also define a useful choice of droop coefficients.
Definition 2: (**Proportional Controller Coefficients**). The controller coefficients (droop coefficients and injections setpoints) are selected proportionally if for all $i, j \in \mathcal{V}_I$

$$P_i^*/D_i = P_j^*/D_j \quad \text{and} \quad P_i^*/\overline{P}_i = P_j^*/\overline{P}_j. \tag{14}$$

A proportional choice of controller coefficients leads to a fair load sharing among the inverters according to their ratings and subject to actuation constraints [15, Theorem 7]:

Theorem 3.3: (**Power Flow Constraints and Power Sharing**). Consider an equilibrium manifold $[\theta^*] \subset \mathbb{T}^n$ of the shifted control system (9) with proportional controller coefficients. The following statements are equivalent:

(i) **Injection constraints:** $0 \leq P_{e,i}(\theta^*) \leq \overline{P}_i, \quad \forall i \in \mathcal{V}_I$;
(ii) **Serviceable load:** $0 \leq -\sum_{i\in\mathcal{V}_L} P_i^* \leq \sum_{j\in\mathcal{V}_I} \overline{P}_j$.
Moreover, the inverters share the total load $\sum_{i\in\mathcal{V}_L} P_i^*$ proportionally according to their power ratings.

D. Power Flow Shaping

We now address the following "controllability" question: given a set of desired power injections for the inverters, can one select the droop coefficients to generate these injections?

We define a *power injection setpoint* as a point of power balance, at fixed load demands and subject to the basic feasibility condition given in Theorem 3.2.

Definition 3: (**Feasible Power Injection Setpoint**). Let $\gamma \in [0, \pi/2[$. A vector $P^{\mathrm{set}} \in \mathbb{R}^n$ is a *γ-feasible power injection setpoint* if it satisfies the following three properties:

(i) **Power balance:** $P^{\mathrm{set}} \in \mathbb{1}_n^\perp$;
(ii) **Load invariance:** $P_i^{\mathrm{set}} = P_i^*$ for all loads $i \in \mathcal{V}_L$;
(iii) **γ-feasibility:** the associated branch power flows $\xi^{\mathrm{set}} = B^\dagger P^{\mathrm{set}}$ are feasible, that is, $\|\mathcal{A}^{-1}\xi^{\mathrm{set}}\|_\infty \leq \sin(\gamma)$.

The next result characterizes the relationship between droop control and γ-feasible injection setpoints. For simplicity, we omit the case $\omega_{\mathrm{sync}} = 0$, since in this case the droop coefficients offer no control over the steady-state injections.

Theorem 3.4: (**Power Flow Shaping**). Consider the shifted control system (9). Assume $\omega_{\mathrm{sync}} \neq 0$, let $P^{\mathrm{set}} \in \mathbb{1}_n^\perp$, and let $\gamma \in [0, \pi/2[$. The following statements are equivalent:

(i) **Coefficient selection:** there exists a selection of droop coefficients D_i, $i \in \mathcal{V}_I$, such that the steady-state injections satisfy $P_e(\theta^*) = P^{\mathrm{set}}$, with $[\theta^*] \subset \overline{\Delta}_G(\gamma)$;
(ii) **Feasibility:** P^{set} is a γ-feasible power injection setpoint.
If the equivalent statements (i) and (ii) hold true, then the quantities D_i and P_i^{set} are related with arbitrary $\beta \neq 0$ as

$$D_i = \beta(P_i^* - P_i^{\mathrm{set}}), \quad i \in \mathcal{V}_I. \tag{15}$$

Moreover, $[\theta^*]$ is locally exponentially stable if and only if $\beta(P_i^* - P_i^{\mathrm{set}})$ is nonnegative for all $i \in \mathcal{V}_I$.

Proof: **(i) $\Longrightarrow$ (ii):** Since $\theta^* \in \overline{\Delta}_G(\gamma)$ and $P_e(\theta^*) \in \mathbb{1}_n^\perp$, Theorem 3.2 shows that P^{set} is a γ-feasible setpoint.

(ii) $\Longrightarrow$ (i): Let P^{set} be a γ-feasible setpoint. Consider the droop coefficients $D_i = \beta(P_i^* - P_i^{\mathrm{set}})$. Since $\omega_{\mathrm{sync}} \neq 0$, for each $i \in \mathcal{V}_I$ we obtain the steady-state injection

$$P_{e,i}(\theta^*) = \widetilde{P}_i = P_i^* - D_i\omega_{\mathrm{sync}}$$

$$= P_i^* - \beta(P_i^* - P_i^{\mathrm{set}})\frac{1}{\beta}\underbrace{\frac{\sum_{i\in\mathcal{V}} P_i^*}{\sum_{i\in\mathcal{V}_I}(P_i^* - P_i^{\mathrm{set}})}}_{=1} = P_i^{\mathrm{set}},$$

where we used $\sum_{i\in\mathcal{V}_I} P_i^{\text{set}} = -\sum_{i\in\mathcal{V}_L} P_i^*$. Since $P_{\text{e},i}(\theta^*) = P_i^* = P_i^{\text{set}}$ for each $i \in \mathcal{V}_L$, we have $\overline{P}_{\text{e}}(\theta) = P^{\text{set}}$. Since P^{set} is γ-feasible, θ^* is well defined in $\overline{\Delta}_G(\gamma)$. By the Jacobian arguments leading to [15, Theorem 2], the shifted system (9) is stable if and only if all D_i are nonnegative. $\square$

By Theorem 3.4, the set of feasible setpoints is in *one-to-one* correspondence with the steady-states reachable by droop control. We refer to [1] for a modification on how to include the injection constraint $P_i^{\text{set}} \in [0, \overline{P}_i]$.

IV. DISTRIBUTED SECONDARY CONTROL STRATEGIES

Primary droop control (4) results in the static frequency error ω_{sync} in (5). The purpose of the secondary control $u_i(t)$ in (6) is to eliminate this static error despite unknown loads.

A. Decentralized Secondary Integral Control

We partition the set of inverters as $\mathcal{V}_I = \mathcal{V}_{I_P} \cup \mathcal{V}_{I_S}$, where the action of the $\mathcal{V}_{I_P}$ inverters is restricted to primary droop control, and the $\mathcal{V}_{I_S}$ inverters perform the secondary control:

$$D_i\dot{\theta}_i = P_i^* - P_{\text{e},i}(\theta), \qquad i \in \mathcal{V}_{I_P}, \qquad (16a)$$
$$D_i\dot{\theta}_i = P_i^* - P_{\text{e},i}(\theta) + u_i(t), \qquad i \in \mathcal{V}_{I_S}. \qquad (16b)$$

Assume that each of the $\mathcal{V}_{I_S}$ inverters uses decentralized integral control to suppress the steady-state frequency error:

$$u_i(t) = -p_i \ , \ \ k_i\dot{p}_i = \dot{\theta}_i, \qquad i \in \mathcal{V}_{I_S}, \qquad (17)$$

For $|\mathcal{V}_{I_S}| = 1$ (mimicking AGC in transmission networks), if a steady-state exists, then $\dot{\theta}_i$ must converge to zero and p_i to the total power imbalance $\sum_{i\in\mathcal{V}} P_i^*$. Hence, the control (17) can achieve frequency regulation, but it fails to maintain load sharing and places a large burden on a single source.

For $|\mathcal{V}_{I_S}| \geq 2$, the control (17) results in a set of invariant closed-loop subspaces corresponding to different choices of u^* rendering ω_{sync}^* to zero; see (7). One way to remove these subspaces is to implement (17) via the low-pass filter

$$u_i(t) = -p_i \ , \ \ k_i\dot{p}_i = \dot{\theta}_i - \epsilon p_i, \qquad i \in \mathcal{V}_{I_S}, \qquad (18)$$

For small $\epsilon > 0$ and large $k \gg 1$ (enforcing a time-scale separation), the controller (18) achieves practical stabilization but does not exactly regulate the frequency [10]. In conclusion, the decentralized control (17) and its variations generally fail to achieve fast frequency regulation while maintaining load sharing. Additionally, a single microgrid source may not have the authority or the capacity to perform secondary control.

B. Distributed Averaging PI (DAPI) Control

As an alternative secondary control strategy, consider the *distributed averaging PI* (DAPI) controller [15]:

$$u_i = -p_i \ , \ \ k_i\dot{p}_i = D_i\dot{\theta}_i + \sum_{j\in\mathcal{V}_{I_S}} L_{ij}\left(\frac{p_i}{D_i} - \frac{p_j}{D_j}\right). \quad (19)$$

Here, we assume that $k_i > 0$, $|\mathcal{V}_{I_S}| \geq 2$, and L is the Laplacian of a weighted, connected and undirected communication graph between the $\mathcal{V}_{I_S}$ inverters. The following result shows that, for any choice of gains $D_i > 0$ and $k_i > 0$, the DAPI control (2), (16), (19) stabilizes the closed loop, regulates the network frequency, and preserves the injections established by the primary control. For simplicity, we only present the result for $\mathcal{V}_{I_S} = \mathcal{V}_I$ proved in [15, Theorem 8]. The extended case $\mathcal{V}_{I_S} \subsetneq \mathcal{V}_I$ is analyzed in [1], [13]. In the latter case, the load sharing is recovered only among the $\mathcal{V}_{I_S}$ inverters.

Theorem 4.1: (**Stability of DAPI-Controlled Network**). Consider the DAPI-controlled microgrid (2), (16), (19) with parameters $P_i^* \in [0, \overline{P}_i]$, $D_i, k_i > 0$ for all $i \in \mathcal{V}_I$, with $\mathcal{V}_{I_S} = \mathcal{V}_I$, and with a connected communication graph among the inverters $\mathcal{V}_I$. The following statements are equivalent:

(i) **Stability of primary droop control:** the droop control stability condition (12) holds;
(ii) **Stability of secondary DAPI control:** there exists an arc length $\gamma \in [0, \pi/2[$ such that the closed loop (2), (16), (19) possesses a locally exponentially stable and unique equilibrium manifold $([\theta^*], p^*) \subset \overline{\Delta}_G(\gamma) \times \mathbb{R}^{n_I}$.

If the equivalent statements (i) and (ii) hold true, then $[\theta^*]$ is given as in Theorem 3.2, and $p_i^* = D_i\omega_{\text{sync}}$ for $i \in \mathcal{V}_I$.

It is interesting to note that the DAPI control can also be applied to the conventional AGC case [18], and it has been independently derived for parallel (star) topologies [21] as a continuous-time demand response strategy. Finally, variations of the DAPI control (19) with similar performance but other signal flows (e.g., additionally integrating edge flows) can also be derived from the perspectives of network flow optimization [22], [28] or dynamic consensus [29], [30].

V. DECENTRALIZED TERTIARY CONTROL STRATEGIES

In this section, we examine the tertiary control layer. Similar to load sharing or flow shaping, we show that the AC economic dispatch (8) can be minimized by droop control.

A. Convex Reformulation of the AC Economic Dispatch

The AC economic dispatch (8) is a non-convex problem due to the nonlinear AC injections entering in the constraints. In practical system operation, the nonlinear AC injections $P_{\text{e},i}(\theta)$ are often approximated by the linear *DC injections*

$$P_{\text{DC},i}(\theta) = \sum_{j=1}^{n} \mathfrak{Im}(Y_{ij}) E_i E_j (\theta_i - \theta_j), \qquad i \in \mathcal{V}. \quad (20)$$

Accordingly, the AC economic dispatch (8) is approximated by the corresponding *DC economic dispatch* given by

$$\underset{\delta\in\mathbb{R}^n, v\in\mathbb{R}^{n_I}}{\text{minimize}} \quad f(v) = \sum_{i\in\mathcal{V}_I} \frac{1}{2}\alpha_i v_i^2 \qquad\qquad (21a)$$
$$\text{subject to} \qquad P_i^* + v_i = P_{\text{DC},i}(\delta) \qquad \forall\, i \in \mathcal{V}_I, \quad (21b)$$
$$P_i^* = P_{\text{DC},i}(\delta) \qquad \forall\, i \in \mathcal{V}_L, \quad (21c)$$
$$|\delta_i - \delta_j| \leq \gamma_{ij}^{(\text{DC})} \qquad \forall\, \{i,j\} \in \mathcal{E}, \quad (21d)$$
$$P_{\text{DC},i}(\delta) \in [0, \overline{P}_i] \qquad \forall\, i \in \mathcal{V}_I, \quad (21e)$$

where the DC variables (δ, v) are distinguished from the AC variables (θ, u). In formulating the DC economic dispatch (21), we also changed the line flow parameters from $\gamma_{ij}^{(\text{AC})}$ to $\gamma_{ij}^{(\text{DC})} \in [0, \pi/2[$ for all $\{i,j\} \in \mathcal{E}$. The DC dispatch (21) is a quadratic program with linear constraints and hence convex.

Typically, the solution (δ^*, v^*) of the DC dispatch (21) serves as proxy for the solution of the non-convex AC dispatch (8). The following result shows that both problems are equivalent for acyclic networks and appropriate constraints.

Theorem 5.1: (**Equivalence of AC and DC Economic Dispatch in Acyclic Networks**). Consider the AC economic dispatch (8) and the DC economic dispatch (21) in an acyclic network. The following statements are equivalent:

(i) *AC feasibility:* the AC economic dispatch problem (8) with parameters $\gamma_{ij}^{(AC)} < \pi/2$ for all $\{i,j\} \in \mathcal{E}$ is feasible with a global minimizer $(\theta^*, u^*) \in \mathbb{T}^n \times \mathbb{R}^{n_I}$;

(ii) *DC feasibility:* the DC economic dispatch problem (21) with parameters $\gamma_{ij}^{(DC)} < 1$ for all $\{i,j\} \in \mathcal{E}$ is feasible with a global minimizer $(\delta^*, v^*) \in \mathbb{R}^n \times \mathbb{R}^{n_I}$.

If the equivalent statements (i) and (ii) are true, then $\sin(\gamma_{ij}^{(AC)}) = \gamma_{ij}^{(DC)}$, $u^* = v^*$, $\sin(B^T\theta^*) = B^T\delta^*$, and $f(u^*) = f(v^*)$ is a global minimum.

Proof: Denote the unique vector of AC branch power flows by $\xi = \mathcal{A}\sin(B^T\theta)$; see (11). For an acyclic network, we have $\ker(B) = \emptyset$, and $\xi \in \mathbb{R}^{n-1}$ can be equivalently rewritten as $\xi = \mathcal{A}B^T\delta$ for some $\delta \in \mathbb{R}^n$. Thus, we obtain

$$\mathcal{A}\sin(B^T\theta) = \mathcal{A}B^T\delta. \qquad (22)$$

Now, we associate δ with the angles of the DC flow (20), so that (22) is a *bijective map* between the AC and DC flows.

Due to the AC security constraints (8d), the sine is invertible. If the DC security constraints (21d) satisfy $\|B^T\delta\|_\infty \leq \max_{\{i,j\}\in\mathcal{E}} \gamma_{ij}^{(DC)} < 1$, then $B^T\theta$ can be uniquely recovered from (and mapped to) $B^T\delta$ via (22). Additionally, up to rotational symmetry and modulo 2π, the angle θ and be uniquely recovered from (and mapped to) δ. Thus, identity (22) between the AC and the DC flow serves as a *bijective change of variables* (modulo 2π and up to rotational symmetry). This change of variables maps the AC dispatch (8) to the DC dispatch (21) as follows. The AC injections $P_e(\theta)$ are replaced by the DC injections $P_{DC}(\delta)$. The AC security constraint (8d) translates uniquely to the DC constraint (21d) with $\gamma_{ij}^{(DC)} = \sin(\gamma_{ij}^{(AC)}) < 1$. The AC injection constraint (8e) is mapped to the DC injection constraint (21e).

Finally, if both problems (8) and (21) are feasible with minimizers $u^* = v^*$ and $\sin(B^T\theta^*) = B^T\delta^*$, then $f(u^*) = f(v^*)$ is the global minimum due to convexity of (21). $\square$

Theorem 5.1 relies on the bijection (22) between AC and DC flows in acyclic networks [26], [27]. For cyclic networks, the two problems (8) and (21) are generally not equivalent, but the DC flow is a well-accepted proxy for the AC flow.

We now state a rather surprising result: any minimizer of the AC economic dispatch (8) can be achieved by appropriately designed droop control (4). Conversely, any steady state of the droop-controlled microgrid (2),(4) is the minimizer of an AC economic dispatch (8) with appropriately chosen parameters. The following theorem makes this idea precise for strictly feasible minimizers (strictly satisfying the inequality constraints) and strictly positive (stabilizing) droop coefficients. The proof can be extended to the constrained case at the cost of a less explicit relation between the optimization parameters and the (possibly non-positive) droop coefficients.

Theorem 5.2: (**Droop Control & Economic Dispatch**). Consider the AC economic dispatch (8) and the shifted control system (9). The following statements are equivalent:

(i) *Strict feasibility and optimality:* there are parameters $\alpha_i > 0$, $i \in \mathcal{V}_I$, and $\gamma_{ij}^{(AC)} < \pi/2$, $\{i,j\} \in \mathcal{E}$ such that the AC economic dispatch problem (8) is strictly feasible with global minimizer $(\theta^*, u^*) \in \mathbb{T}^n \times \mathbb{R}^{n_I}$.

(ii) *Constrained sync:* there exists $\gamma \in [0, \pi/2[$ and droop coefficients $D_i > 0$, $i \in \mathcal{V}_I$, so that the shifted control system (9) possesses a unique and locally exponentially stable equilibrium manifold $[\theta] \subset \Delta_G(\gamma)$ meeting injection constraints $P_{e,i}(\theta) \in]0, \overline{P}_i[, i \in \mathcal{V}_I$.

If the equivalent statements (i) and (ii) hold true, then $[\theta^*] = [\theta]$, $\gamma = \max_{\{i,j\}\in\mathcal{E}} \gamma_{ij}^{(AC)}$, and for some $\beta > 0$ it holds that

$$D_i = \beta/\alpha_i, \qquad i \in \mathcal{V}_I. \qquad (23)$$

Theorem 5.2, stated for the shifted control system (9), can be equivalently stated for the CAPI or DAPI control systems (by Lemma 3.1). Before proving it, we state a key lemma.

Lemma 5.3: (**Properties of strictly feasible points**). If $(\theta^*, u^*) \in \mathbb{T}^n \times \mathbb{R}^{n_I}$ is a strictly feasible minimizer of the AC economic dispatch (8), then u^* is *sign-definite*, i.e., all u_i^*, $i \in \mathcal{V}_I$, have the same sign. Conversely, any strictly feasible pair $(\theta, u) \in \mathbb{T}^n \times \mathbb{R}^{n_I}$ of the AC economic dispatch (8) with sign-definite u is *inverse optimal* with respect to some $\alpha \in \mathbb{R}^{n_I}_{>0}$: there are coefficients $\alpha_i > 0$, $i \in \mathcal{V}_I$, such that (θ, u) is global minimizer of the AC economic dispatch (8).

Proof: The strictly feasible pairs of (8) are the set of all $(\theta, u) \in \mathbb{T}^n \times \mathbb{R}^{n_I}$ satisfying the power flow equations (8b)-(8c) and the strict inequality constraints (8d)-(8e). Summing all equations (8b)-(8c) yields the necessary solvability condition (power balance constraint) $\sum_{i\in\mathcal{V}_I} u_i = -\sum_{i\in\mathcal{V}} P_i^*$.

To establish the necessary and sufficient optimality conditions in the strictly feasible case, without loss of generality, we drop the inequality constraints (8d)-(8e). With $\lambda \in \mathbb{R}^n$, the Lagrangian $\mathcal{L} : \mathbb{T}^n \times \mathbb{R}^{n_I} \times \mathbb{R}^n \to \mathbb{R}$ is

$$\mathcal{L}(\theta, u, \lambda) = \sum_{j\in\mathcal{V}_I} \frac{1}{2}\alpha_j u_j^2 + \sum_{j\in\mathcal{V}_I} \lambda_j \left(u_j + P_j^* - P_{e,j}(\theta)\right)$$
$$+ \sum_{j\in\mathcal{V}_L} \lambda_j \left(P_j^* - P_{e,j}(\theta)\right).$$

The necessary KKT conditions for optimality are:

$$\frac{\partial\mathcal{L}}{\partial\theta_i} = 0 : \quad 0 = \sum_{j\in\mathcal{V}} \lambda_j \cdot \frac{\partial P_{e,j}(\theta)}{\partial\theta_i}, \quad \forall i \in \mathcal{V}, \quad (24a)$$

$$\frac{\partial\mathcal{L}}{\partial u_i} = 0 : \quad \alpha_i u_i = -\lambda_i, \qquad\qquad \forall i \in \mathcal{V}_I, \quad (24b)$$

$$\frac{\partial\mathcal{L}}{\partial\lambda_i} = 0 : \quad -u_i = P_i^* - P_{e,i}(\theta), \qquad \forall i \in \mathcal{V}_I, \quad (24c)$$

$$\frac{\partial\mathcal{L}}{\partial\lambda_i} = 0 : \quad 0 = P_i^* - P_{e,i}(\theta), \qquad\quad \forall i \in \mathcal{V}_L. \quad (24d)$$

Since the AC dispatch (8) is equivalent to the convex DC dispatch (see Theorem 5.1), the KKT conditions (24) are also sufficient for optimality. In vector form, (24a) reads as $\mathbf{0}_n = \lambda^\mathsf{T} \partial P_e(\theta)/\partial\theta$, where the *load flow Jacobian* is given by symmetric Laplacian $\partial P_e(\theta)/\partial\theta = B \operatorname{diag}(\{a_{ij}\}_{\{i,j\}\in\mathcal{E}}) B^T$ with strictly positive weights $a_{ij} = \mathfrak{Im}(Y_{ij})E_iE_j \cos(\theta_i - \theta_j)$ (due to strict feasibility of the security constraint (8d)).

It follows that $\lambda \in \mathbb{1}_n$, that is, $\lambda_i = \widetilde{\lambda} \in \mathbb{R}$ for all $i \in \mathcal{V}$ and for some $\widetilde{\lambda} \in \mathbb{R}$. Hence, condition (24b) reduces to $u_i\alpha_i = \widetilde{\lambda}$ for all $i \in \mathcal{V}_I$, that is, all marginal utilities must

be identical which is also known as the *economic dispatch criterion* [9]. Conditions (24c)-(24d) then reduce to

$$\widetilde{\lambda}/\alpha_i = P_i^* - P_{\mathrm{e},i}(\theta), \qquad \forall i \in \mathcal{V}_I, \tag{25a}$$

$$0 = P_i^* - P_{\mathrm{e},i}(\theta), \qquad \forall i \in \mathcal{V}_L. \tag{25b}$$

By summing all equations (25), we obtain the constant $\widetilde{\lambda} = \sum_{i \in \mathcal{V}} P_i^* / \sum_{i \in \mathcal{V}_\mathcal{I}} \alpha_i^{-1}$. The minimizers are $u_i^* = -\widetilde{\lambda}/\alpha_i$ and θ^* determined from (25). It follows that u^* is sign-definite.

By comparing the (strict) optimality conditions (25) with the (strict) feasibility conditions (8b)-(8c), it follows that any strictly feasible pair (θ, u) with sign-definite u is inverse optimal for the coefficients $\alpha_i = -\beta/u_i$ with some $\beta > 0$. $\square$

Proof of Theorem 5.2: **(i)** $\implies$ **(ii):** If the AC economic dispatch (8) is strictly feasible, then its minimizer (θ^*, u^*) is global (Theorem 5.1), and the optimal inverter injections are $P_i^{\mathrm{opt}} = P_{\mathrm{e},i}(\theta^*) = P_i^* + u_i^*$ with sign-definite u^* (Lemma 5.3). Since the power flow equations (8b)-(8c) and the strict inequality constraints (8d)-(8e) are met, $P_i^{\mathrm{opt}} \in \,]0, \overline{P}_i[$, $[\theta^*] \subset \Delta_G(\gamma)$ with $\gamma = \max_{\{i,j\} \in \mathcal{E}} \gamma_{ij}^{(\mathrm{AC})}$, and the vector of injections $(P_L^*, P_I^{\mathrm{opt}})$ is a γ-feasible injection setpoint.

By Theorem 3.4 and identity (15), the droop coefficients $D_i = -\beta(P_i^* - P_i^{\mathrm{opt}}) = \beta u_i^*$, $i \in \mathcal{V}_I$, guarantee that the shifted control system (9) possesses an equilibrium manifold $[\theta]$ satisfying $P_{\mathrm{e}}(\theta) = P^{\mathrm{set}} = P_{\mathrm{e}}(\theta^*)$. For $\beta u_i^* > 0$ (recall u^* is sign-definite), $[\theta]$ is locally exponentially stable by Theorem 3.2. Finally, $[\theta^*] = [\theta]$ since $P_{\mathrm{e}}(\theta) = P_{\mathrm{e}}(\theta^*)$.

(ii) $\implies$ **(i):** Any equilibrium manifold $[\theta] \subset \Delta_G(\gamma)$ as in (ii) is a γ-feasible power injection setpoint with

$$\widetilde{P}_i = P_i^* - D_i \omega_{\mathrm{sync}} = P_{\mathrm{e},i}(\theta) \qquad \forall\, i \in \mathcal{V}_I, \tag{26a}$$

$$\widetilde{P}_i = P_i^* = P_{\mathrm{e},i}(\theta) \qquad \forall\, i \in \mathcal{V}_L, \tag{26b}$$

$$|\theta_i - \theta_j| < \gamma \qquad \forall\, i, j \in \mathcal{E}, \tag{26c}$$

$$P_{\mathrm{e},i}(\theta) \in \,]0, \overline{P}_i[\qquad \forall\, i \in \mathcal{V}_I. \tag{26d}$$

Hence, any $\theta \in [\theta]$ is strictly feasible for the economic dispatch (8) if we identify θ^* with θ (modulo symmetry), γ with $\max_{\{i,j\} \in \mathcal{E}} \gamma_{ij}^{(\mathrm{AC})}$, and u_i^* with $-D_i \omega_{\mathrm{sync}}$ (modulo scaling). Since u_i^* is sign-definite, the claim follows from Lemma 5.3.

Finally, a comparison of the stationarity conditions (26a)-(26b) and the optimality conditions (25) gives $D_i \omega_{\mathrm{sync}} = -u_i^* = \widetilde{\lambda}/\alpha_i$, where ω_{sync} and $\widetilde{\lambda}$ are constant. Since the droop gains are defined up to scaling, we obtain (23). $\square$

The equivalence revealed in Theorem 5.2 suggests the following guidelines to select the droop coefficients: choose D_i large for desirable (e.g., economic or low emission) sources with small marginal costs α_i; and vice versa. These insights can also be connected to the objective of proportional load sharing: if each P_i^* and $1/\alpha_i$ are selected proportional to the rating $\overline{P}_i$, that is, $\alpha_i \overline{P}_i = \alpha_j \overline{P}_j$ and $P_i^*/\overline{P}_i = P_j^*/\overline{P}_j$, then the associated droop coefficients (23) equal those in (14).

From an optimization perspective, the primary dynamics (9) serve as a primal algorithm to minimize (8). Likewise, second-order or integral control dynamics serve as primal-dual algorithm, as shown for related systems in [19]–[22], [28], [29]. Indeed, for $\mathcal{V}_{I_S} = \mathcal{V}_I$, the DAPI controller (2), (16), (19) can be derived as a primal-dual interior point method to solve the AC economic dispatch (8), see [21, equation (6)] in absence of inequality constraints.

VI. Simulation Case Study

We illustrate the performance and robustness of our controllers via a simulation of the IEEE 37 distribution system in Fig. 1(a). After an islanding event, the distribution network is disconnected from the transmission grid, and distributed sources must ensure stability while regulating the frequency and sharing the demand. The cyber layer describing the communication among the distributed generators is shown in dotted blue. Of the 16 sources, 8 have identical power ratings, while the other 8 are rated for twice as much power.

Instead of the lossless power flow (1), we use the full lossy equations. To include reactive power dynamics, the inverter voltages are controlled via the *quadratic voltage-droop* [31]

$$\tau_i \dot{E}_i = -C_i E_i (E_i - E_i^*) - Q_{\mathrm{e},i}, \qquad i \in \mathcal{V}_I,$$

where $E_i^* > 0$ is the nominal voltage, $C_i, \tau_i > 0$ are gains, and $Q_{\mathrm{e},i} \in \mathbb{R}$ is the reactive power injection (1b). Fig. 1(b) and (c) show a comparison between the decentralized secondary controllers (17) implemented at every inverter, and the DAPI controller (19), with equal gains. While both controllers regulate the frequency, the decentralized controllers (17) do not maintain load sharing under a change in load.
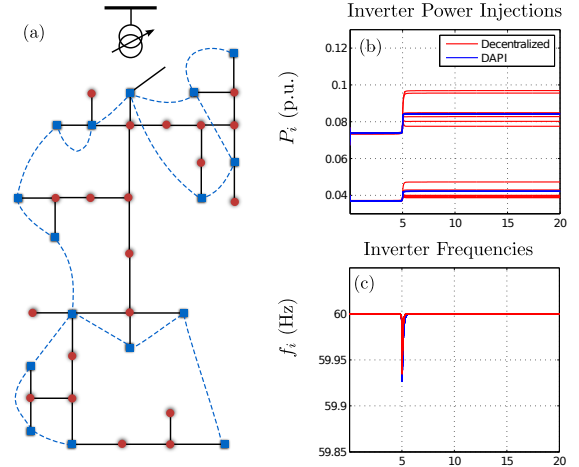

Fig. 1. Comparison of decentralized control (18) and DAPI control (19).

VII. Conclusions

We studied decentralized and distributed primary, secondary, and tertiary control strategies in microgrids and illuminated some connections between them. Thereby, we relaxed some restrictions regarding the information structure and time-scale separation of conventional hierarchical control strategies adapted from bulk power systems to make them applicable to microgrids and distribution-level applications.

While this work is a first step towards an understanding of the interdependent control loops in hierarchical microgrids, several complicating factors have not been taken into account. In particular, our analysis is thus far formally restricted to acyclic networks with lossless (or constant R/X ratio) lines. Moreover, future work needs to consider more detailed models including reactive power flows, voltage dynamics, and ramping constraints on the inverter power injections.

REFERENCES

[1] F. Dörfler, J. W. Simpson-Porco, and F. Bullo, "Breaking the hierarchy: Distributed control & economic optimality in microgrids," *IEEE Transactions on Control of Network Systems*, Jan. 2014, submitted.

[2] R. H. Lasseter, "Microgrids," in *IEEE Power Engineering Society Winter Meeting*, vol. 1, 2002, pp. 305–308.

[3] M. C. Chandorkar, D. M. Divan, and R. Adapa, "Control of parallel connected inverters in standalone AC supply systems," *IEEE Transactions on Industry Applications*, vol. 29, no. 1, pp. 136–143, 1993.

[4] Q.-C. Zhong and T. Hornik, *Control of Power Inverters in Renewable Energy and Smart Grid Integration*. Wiley-IEEE Press, 2013.

[5] J. M. Guerrero, J. C. Vasquez, J. Matas, L. G. de Vicuna, and M. Castilla, "Hierarchical control of droop-controlled AC and DC microgrids–a general approach toward standardization," *IEEE Transactions on Industrial Electronics*, vol. 58, no. 1, pp. 158–172, 2011.

[6] A. Mohd, E. Ortjohann, D. Morton, and O. Omari, "Review of control techniques for inverters parallel operation," *Electric Power Systems Research*, vol. 80, no. 12, pp. 1477–1487, 2010.

[7] J. A. P. Lopes, C. L. Moreira, and A. G. Madureira, "Defining control strategies for microgrids islanded operation," *IEEE Transactions on Power Systems*, vol. 21, no. 2, pp. 916–924, 2006.

[8] J. Machowski, J. W. Bialek, and J. R. Bumby, *Power System Dynamics*, 2nd ed. Wiley, 2008.

[9] A. J. Wood and B. F. Wollenberg, *Power Generation, Operation, and Control*, 2nd ed. Wiley, 1996.

[10] N. Ainsworth and S. Grijalva, "Design and quasi-equilibrium analysis of a distributed frequency-restoration controller for inverter-based microgrids," in *North American Power Symposium*, Manhattan, KS, USA, Sep. 2013.

[11] Q. Shafiee, J. Guerrero, and J. M. Vasquez, "Distributed secondary control for islanded microgrids - a novel approach," *IEEE Transactions on Power Electronics*, 2013, to appear.

[12] H. Liang, B. J. Choi, W. Zhuang, and X. Shen, "Stability enhancement of decentralized inverter control through wireless communications in microgrids," *IEEE Transactions on Smart Grid*, vol. 4, no. 1, pp. 321–331, 2013.

[13] H. Bouattour, J. W. Simpson-Porco, F. Dörfler, and F. Bullo, "Further results on distributed secondary control in microgrids," in *IEEE Conf. on Decision and Control*, Florence, Italy, Dec. 2013, pp. 1514–1519.

[14] L.-Y. Lu, "Consensus-based $P - f$ and $Q - \dot{V}$ droop control for multiple parallel-connected inverters in lossy networks," in *IEEE International Symposium on Industrial Electronics*, Taipei, Taiwan, May 2013.

[15] J. W. Simpson-Porco, F. Dörfler, and F. Bullo, "Synchronization and power sharing for droop-controlled inverters in islanded microgrids," *Automatica*, vol. 49, no. 9, pp. 2603–2611, 2013.

[16] J. W. Simpson-Porco, F. Dörfler, Q. Shafiee, J. M. Guerrero, and F. Bullo, "Stability, power sharing, & distributed secondary control in droop-controlled microgrids," in *IEEE Int. Conf. on Smart Grid Communications*, Vancouver, BC, Canada, Oct. 2013, pp. 672–677.

[17] M. Andreasson, D. V. Dimarogonas, K. H. Johansson, and H. Sandberg, "Distributed vs. centralized power systems frequency control under unknown load changes," in *European Control Conference*, Zürich, Switzerland, Jul. 2013, pp. 3524–3529.

[18] M. Andreasson, D. V. Dimarogonas, H. Sandberg, and K. H. Johansson, "Distributed pi-control with applications to power systems frequency control," *arXiv preprint arXiv:1311.0116*, 2013.

[19] C. Zhao, U. Topcu, N. Li, and S. Low, "Power system dynamics as primal-dual algorithm for optimal load control," *arXiv preprint arXiv:1305.0585*, 2013.

[20] N. Li, L. Chen, C. Zhao, and S. H. Low, "Connecting automatic generation control and economic dispatch from an optimization view," in *American Control Conference*, 2014, submitted.

[21] X. Zhang and A. Papachristodoulou, "A real-time control framework for smart power networks with star topology," in *American Control Conference (ACC), 2013*. IEEE, 2013, pp. 5062–5067.

[22] E. Mallada and S. H. Low, "Distributed frequency-preserving optimal load control," in *IFAC World Congress*, 2014, submitted.

[23] E. Mojica-Nava, C. Macana, and N. Quijano, "Dynamic population games for optimal dispatch on hierarchical microgrid control," *Systems, Man, and Cybernetics: Systems, IEEE Transactions on*, vol. 44, no. 3, pp. 306–317, March 2014.

[24] R. Mudumbai and S. Dasgupta, "Distributed control for the smart grid: the case of economic dispatch," in *Information Theory and Applications*, 2013.

[25] S. T. Cady, A. D. Domínguez-García, and C. N. Hadjicostis, "A distributed generation control architecture for small-footprint power systems," 2013, submitted.

[26] F. Dörfler, M. Chertkov, and F. Bullo, "Synchronization in complex oscillator networks and smart grids," *Proceedings of the National Academy of Sciences*, vol. 110, no. 6, pp. 2005–2010, 2013.

[27] F. Dörfler and F. Bullo, "Novel insights into lossless AC and DC power flow," in *IEEE Power & Energy Society General Meeting*, Vancouver, BC, Canada, Jul. 2013.

[28] M. Bürger, D. Zelazo, and F. Allgöwer, "Duality and network theory in passivity-based cooperative control," *arXiv preprint arXiv:1301.3676*, 2013.

[29] M. Bürger and C. De Persis, "Dynamic coupling design for nonlinear output agreement and time-varying flow control," *arXiv preprint arXiv:1311.7562*, 2013.

[30] H. Bai and S. Y. Shafi, "Output synchronization of nonlinear systems under input disturbances," *arXiv preprint arXiv:1312.6421*, 2013.

[31] J. W. Simpson-Porco, F. Dörfler, and F. Bullo, "Voltage stabilization in microgrids via quadratic droop control," in *IEEE Conf. on Decision and Control*, Florence, Italy, Dec. 2013, pp. 7582–7589.